

A new lyotropic liquid-crystalline phase is formed from oligo-(ethylene oxide) surfactants and  $M(H_2O)_nX_m$  transition metal complexes. Shown are a polarization optical microscopy image demonstrating the fan texture of the hexagonal phase and a schematic representation of the hexagonal phase. For more information see the following pages.

## A New Lyotropic Liquid Crystalline System: Oligo(ethylene oxide) Surfactants with $[M(H_2O)_n]X_m$ Transition Metal Complexes\*\*

Özgür Çelik and Ömer Dag\*

The realization of self-assembling liquid crystalline templating (SLCT) for the synthesis of *meso*-structured materials has attracted great attention from the materials community over the past decade.<sup>[1–16]</sup> The SLCT approach has also made the materials community realize new approaches to the synthesis of materials in the form of powders,<sup>[5]</sup> thin films,<sup>[6]</sup> fibers,<sup>[7]</sup> and even photonic band-gap materials.<sup>[8]</sup> The lyotropic liquid crystalline (LLC) properties and the phase diagrams of many oligo(ethylene oxide)-type surfactants, which are the main focus of our work, have been established in water<sup>[17]</sup> and in the presence of alkali metal salts which complex with the oxyethylene oxide chains.<sup>[18]</sup> The non-ionic oligo(ethylene oxide) surfactants have also been used as templates for the synthesis of mesoporous materials.<sup>[9–15]</sup> Attard et al<sup>[9]</sup> first introduced the synthesis of the oriented monolithic mesoporous silica by using the LC phase-templating approach. Since its introduction, this approach has been applied to the synthesis of nanostructured and mesoporous CdS, CdSe,<sup>[10]</sup> ZnS,<sup>[10, 11]</sup> Pt mesh,<sup>[12]</sup> and CaPO<sub>4</sub>.<sup>[13]</sup> The approach has also been applied to the introduction of LiCF<sub>3</sub>SO<sub>3</sub> and AgNO<sub>3</sub> into mesoporous silica materials.<sup>[14, 15]</sup> However, in all these procedures, the LC phase was first achieved by using the lyotropic property of the oligo(ethylene oxide) in water (typically, 50% w/w water/surfactant mixture and with a low concentration of the additives, such as H<sub>2</sub>[PtCl<sub>6</sub>] (the phase diagrams have also been constructed),<sup>[16]</sup> LiCF<sub>3</sub>SO<sub>3</sub>, AgNO<sub>3</sub>, CdX<sub>n</sub> (X = Cl<sup>-</sup>, SO<sub>4</sub><sup>2-</sup>, NO<sub>3</sub><sup>-</sup>, and CH<sub>3</sub>COO<sup>-</sup>), and Zn(NO<sub>3</sub>)<sub>2</sub>).<sup>[10–16]</sup> In the majority of these studies it was established that the metal salt concentration must be low to maintain the LC phase during further processing of the mixtures.<sup>[10–15]</sup>

Here we report that the assemblies formed between non-ionic oligo(ethylene oxides) surfactants C<sub>12</sub>H<sub>25</sub>-(CH<sub>2</sub>CH<sub>2</sub>O)<sub>10</sub>OH (N<sup>o</sup>) with transition metal aqua complex salts (such as [Co(H<sub>2</sub>O)<sub>6</sub>](NO<sub>3</sub>)<sub>2</sub>, [Ni(H<sub>2</sub>O)<sub>6</sub>](NO<sub>3</sub>)<sub>2</sub>, [Zn(H<sub>2</sub>O)<sub>6</sub>](NO<sub>3</sub>)<sub>2</sub>, and [Cd(H<sub>2</sub>O)<sub>4</sub>](NO<sub>3</sub>)<sub>2</sub> (MX<sub>2</sub>)) have LC behavior at various MX<sub>2</sub>/N<sup>o</sup> mole ratios. The transition metal aqua complexes, which induce the oligo(ethylene oxide) surfactants to undergo self-assembly into a LC phase, act as the second component of the LLC. The concentration range for various MX<sub>2</sub> salts, the isotropization temperatures (ITs), and the effect of the counterion on the IT in these mixtures were determined.

Various MX<sub>2</sub>/N<sup>o</sup> mixtures were prepared in order to study the behavior of the LC phase of non-ionic surfactants in the

presence of NO<sub>3</sub><sup>-</sup> salts of [Ni(H<sub>2</sub>O)<sub>6</sub>]<sup>2+</sup>, [Co(H<sub>2</sub>O)<sub>6</sub>]<sup>2+</sup>, [Zn(H<sub>2</sub>O)<sub>6</sub>]<sup>2+</sup>, and [Cd(H<sub>2</sub>O)<sub>4</sub>]<sup>2+</sup> ions. The Cl<sup>-</sup> and SO<sub>4</sub><sup>2-</sup> salts of these transition metal aqua complexes do not dissolve in this surfactant and therefore no LC phase could be observed. However, [Co(H<sub>2</sub>O)<sub>6</sub>]Cl<sub>2</sub>, which is the only exception, behaves in a similar way to that of NO<sub>3</sub><sup>-</sup> salts. Interestingly, we found that [Co(H<sub>2</sub>O)<sub>6</sub>]Cl<sub>2</sub> undergoes exchange reactions to form the CoCl<sub>4</sub><sup>2-</sup> ion in the [Co(H<sub>2</sub>O)<sub>6</sub>]Cl<sub>2</sub>/N<sup>o</sup> mixture. A color change from reddish pink to sharp blue, which is the typical color of the CoCl<sub>4</sub><sup>2-</sup> ion, is observed upon mixing the [Co(H<sub>2</sub>O)<sub>6</sub>]Cl<sub>2</sub> complex with the non-ionic surfactant.<sup>[19]</sup> The formation of the CoCl<sub>4</sub><sup>2-</sup> ion has also been investigated by UV/Vis-Near IR spectroscopy and will be discussed elsewhere.

A typical polarized-light optical microscopy (POM) image between the crossed polars is shown in Figure 1a. The POM image, which is representative of the hexagonal LC phase of

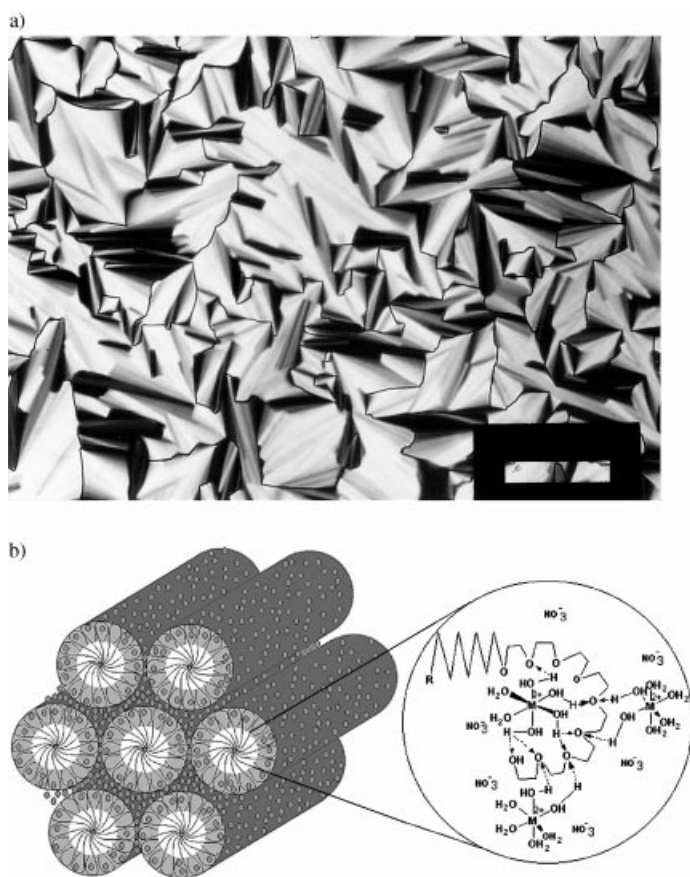


Figure 1. a) A representative POM image of [Cd(H<sub>2</sub>O)<sub>4</sub>](NO<sub>3</sub>)<sub>2</sub> in C<sub>12</sub>H<sub>25</sub>(CH<sub>2</sub>CH<sub>2</sub>O)<sub>10</sub>OH with a MX<sub>2</sub>/N<sup>o</sup> mole ratio of 2.0/1 (the scale bar is 200 μm). b) A schematic representation of a hexagonal LC MX<sub>2</sub>/N<sup>o</sup> structure, the small circles represent [M(H<sub>2</sub>O)<sub>n</sub>]<sup>2+</sup> and NO<sub>3</sub><sup>-</sup> ions.

oligo(ethylene oxide)-type surfactants, displays a fan texture within the MX<sub>2</sub>/N<sup>o</sup> mole ratio range 1.2/1–3.2/1 (which corresponds to 22.2–43.2% w/w for [Co(H<sub>2</sub>O)<sub>6</sub>]Cl<sub>2</sub>/N<sup>o</sup> and 27.0–49.7% w/w for [Cd(H<sub>2</sub>O)<sub>4</sub>](NO<sub>3</sub>)<sub>2</sub>/N<sup>o</sup>) at RT. A schematic representation of the hexagonal structure is shown in Figure 1b. The thermal properties were studied and the IT values for a broad range of MX<sub>2</sub>/N<sup>o</sup> mole ratios were

[\*] Prof. Dr. Ö. Dag, Ö. Çelik  
Bilkent University  
Department of Chemistry  
06533, Ankara (Turkey)  
Fax: (+90)312-290-4579  
E-mail: dag@fen.bilkent.edu.tr

[\*\*] This work was supported by a University Faculty Grant from Bilkent University.

determined (Figure 2). Interestingly, the LC phase of the mixture becomes more stable upon increasing the  $\text{MX}_2/\text{N}^\circ$  mole ratio (Figure 2). Above a critical mole ratio, the IT does not change much from sample to sample for  $\text{Ni}^{\text{II}}$  and  $\text{Co}^{\text{II}}$  complexes. The mixtures of these two complexes are liquid

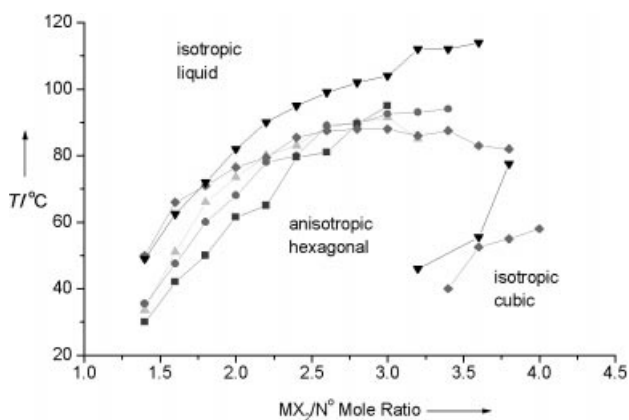


Figure 2. A plot of the isotropization temperatures of the mixtures of  $\text{MX}_2$  and  $\text{C}_{12}\text{H}_{25}(\text{CH}_2\text{CH}_2\text{O})_{10}\text{OH}$  versus the  $\text{MX}_2/\text{N}^\circ$  mole ratios:  $\blacktriangledown$   $[\text{Cd}(\text{H}_2\text{O})_4](\text{NO}_3)_2$ ,  $\blacklozenge$   $[\text{Zn}(\text{H}_2\text{O})_6](\text{NO}_3)_2$ ,  $\blacktriangle$   $[\text{Ni}(\text{H}_2\text{O})_6](\text{NO}_3)_2$ ,  $\bullet$   $[\text{Co}(\text{H}_2\text{O})_6](\text{NO}_3)_2$ ,  $\blacksquare$   $[\text{Co}(\text{H}_2\text{O})_6]\text{Cl}_2$  (mole ratio axis corresponds to 23.6–58.1% w/w for  $[\text{Cd}(\text{H}_2\text{O})_4](\text{NO}_3)_2/\text{N}^\circ$  and 19.1–51.7% w/w for  $[\text{Co}(\text{H}_2\text{O})_6]\text{Cl}_2/\text{N}^\circ$ ).

crystalline and stable up to a  $\text{MX}_2/\text{N}^\circ$  mole ratio of 3.5/1 (ca. 50.5% w/w), and have a fan texture when observed between cross polars. However, the samples with high mole ratios (2.5 and above) undergo slow recrystallization to yield the  $\text{Ni}^{\text{II}}$  and  $\text{Co}^{\text{II}}$  salts.

The  $\text{MX}_2/\text{N}^\circ$  mixtures (where  $\text{MX}_2$  is  $[\text{Zn}(\text{H}_2\text{O})_6](\text{NO}_3)_2$  or  $[\text{Cd}(\text{H}_2\text{O})_4](\text{NO}_3)_2$ ) are even more stable: it is possible to increase the  $\text{MX}_2/\text{N}^\circ$  mole ratio up to 5/1 and 6.5/1 (ca. 59.8 and 62.8% w/w), respectively. The POM images of the  $[\text{Cd}(\text{H}_2\text{O})_4](\text{NO}_3)_2/\text{N}^\circ$  systems above a 3.2/1 mole ratio do not show the hexagonal fan texture at room temperature (RT). Even at a 6.5/1 mole ratio, the  $[\text{Cd}(\text{H}_2\text{O})_4](\text{NO}_3)_2/\text{N}^\circ$  sample is still in a gel phase (highly viscous and transparent, with no fluidity), optically isotropic, and there is no recrystallization of the  $[\text{Cd}(\text{H}_2\text{O})_4](\text{NO}_3)_2$  salt in the mixture if the mixture is kept in a closed container. A sample with a  $[\text{Cd}(\text{H}_2\text{O})_4](\text{NO}_3)_2/\text{N}^\circ$  mole ratio of 3.2/1 (ca. 49.7% w/w) has two phases, the highly viscous (most likely cubic) phase (between RT and 42.5 °C) and the anisotropic phase (with a fan-shaped focal conic texture, which is representative of a columnar hexagonal phase, in the POM image obtained between 42.5 to 113 °C). The cubic to columnar hexagonal phase transition temperature increases with increasing  $[\text{Cd}(\text{H}_2\text{O})_4](\text{NO}_3)_2/\text{N}^\circ$  mole ratios, and reaches approximately 78 °C at a 3.8/1 mole ratio. The  $[\text{Cd}(\text{H}_2\text{O})_4](\text{NO}_3)_2/\text{N}^\circ$  samples decompose over 115 °C above this mole ratio (Figure 2). The samples at higher  $[\text{Cd}(\text{H}_2\text{O})_4](\text{NO}_3)_2/\text{surfactant}$  mole ratios (above 3.2) display one diffraction line around 50 Å  $d$  spacing. However, this optically isotropic phase does not show any anisotropy upon shearing under POM and the samples are highly viscous; these properties are good indications for the existence of a cubic phase.<sup>[20]</sup>

The  $[\text{Ni}(\text{H}_2\text{O})_6](\text{NO}_3)_2$  and  $[\text{Co}(\text{H}_2\text{O})_6](\text{NO}_3)_2$  samples with a  $\text{MX}_2/\text{N}^\circ$  mole ratio above 3.0/1 undergo recrystallization and there is no sample of these two metal complexes with a cubic phase at RT. The POM images of samples at higher  $\text{MX}_2/\text{N}^\circ$  mole ratios always show the characteristic fan texture and the  $\text{MX}_2$  salt crystals. The  $\text{MX}_2/\text{N}^\circ$  mole ratio of 3.0/1 (ca. 46.5% w/w) is most likely the saturation point. Above this ratio, crystallization of the  $\text{MX}_2$  salt complexes ( $[\text{Ni}(\text{H}_2\text{O})_6](\text{NO}_3)_2$  and  $[\text{Co}(\text{H}_2\text{O})_6](\text{NO}_3)_2$ ) takes place. Even at a lower concentration, such as below a 3.0/1 mole ratio, the  $[\text{Ni}(\text{H}_2\text{O})_6](\text{NO}_3)_2$  and  $[\text{Co}(\text{H}_2\text{O})_6](\text{NO}_3)_2$  crystals have been observed after several months of the sample being rested in a closed container. However, heating the crystallized samples to their ITs recovers the LC phase without any  $\text{MX}_2$  crystals.

A set of XRD patterns were recorded on both oriented and unoriented samples (Figure 3) to establish the existence of the *meso*-phase and the structure type. The XRD pattern of the mixtures usually displays the first three lines at around 48, 28,

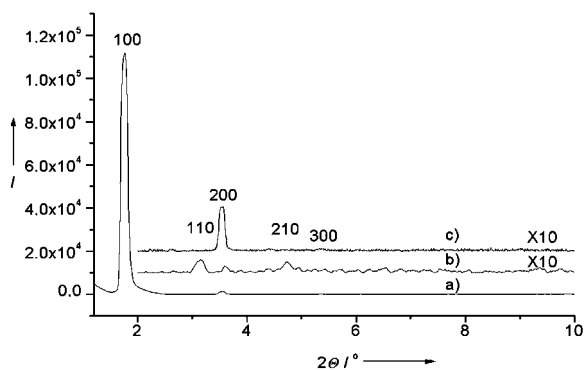


Figure 3. Typical XRD patterns of the oriented  $[\text{Ni}(\text{H}_2\text{O})_6](\text{NO}_3)_2/\text{C}_{12}\text{H}_{25}(\text{CH}_2\text{CH}_2\text{O})_{10}\text{OH}$  sample with a  $\text{MX}_2/\text{N}^\circ$  mole ratio of 1.8/1 (a and c) and an unoriented sample of the same composition (b).

and 24 Å  $d$  spacings, which correspond to the (100), (110), and (200) planes of a 2D-hexagonal phase (with a lattice parameter  $a$  of 55.4 Å). Some samples display up to five diffraction lines corresponding to (100), (110), (200), (210), and (300) planes of the 2D-hexagonal phase (Figure 3). The samples were run in a 0.5-mm deep glass powder X-ray diffraction (PXRD) sample holder by making 0.5-mm-thick films. Heating and cooling the samples several times between the IT and RT, respectively, enabled preparation of the film samples. However, the heating/cooling cycle makes the samples highly oriented. As a result, the (100), (200), and (300) diffraction lines are intense and in general the other lines are invisible. The samples packed without heating/cooling cycles (unoriented samples) display a strong (100) line with relatively weak (110), (200), and (210) lines, but the intensity of the (100) line of the unoriented samples is much weaker than that of the oriented samples. Ozin and co-workers as well as Miyata and Kuroda also observed a similar behavior in their oriented mesoporous silica film samples.<sup>[21]</sup> They observed that while the film samples (oriented) display (100) and (200) diffraction lines, their crushed (powdered) samples show the (100), (110), and (200) diffraction lines corresponding to the hexagonal symmetry.<sup>[21]</sup>

The Vis/Near-IR absorption spectra of a series of  $[\text{Ni}(\text{H}_2\text{O})_6]^{2+}$  and  $[\text{Co}(\text{H}_2\text{O})_6]^{2+}$  complex ions proves that there is no ligand substitution reaction taking place between the surfactant molecules and the aqua complexes. The spectra were recorded in the 400–1400 nm region for  $[\text{Ni}(\text{H}_2\text{O})_6]^{2+}$  and  $[\text{Co}(\text{H}_2\text{O})_6]^{2+}$  at various concentrations in the LC phase and in pure water. The characteristic d–d transitions of these two complexes show no changes in the Vis/Near-IR region other than an increasing intensity with increasing metal aqua complex concentration. This observation indicates that there is no chemical interaction between the surfactant ethylene oxide (EO) groups and the metal center of the aqua complexes (that is, water molecules stay in the coordination sphere).

FT-IR spectroscopy has been used extensively to elucidate the local structural changes in LC mixtures with increasing  $\text{MX}_2/\text{N}^\circ$  mole ratios. The general trend is that the FT-IR spectra of  $[\text{M}(\text{H}_2\text{O})_n]\text{X}_m$  in surfactants display drastic changes around 1200–1500  $\text{cm}^{-1}$  and 900–1100  $\text{cm}^{-1}$ , the  $\nu$ -CO stretching region (Figure 4). The peaks at around 1000–1100  $\text{cm}^{-1}$ , which corresponds to the C–O stretching region

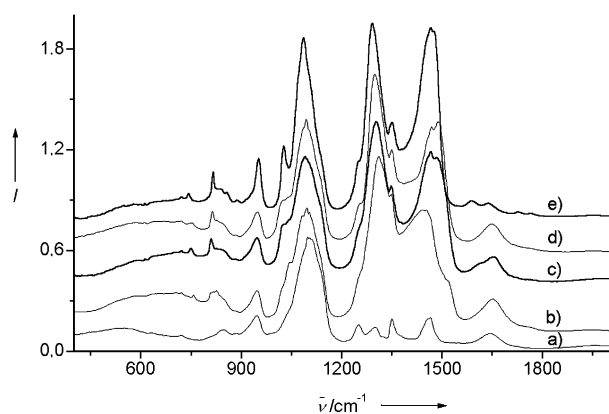


Figure 4. FT-IR spectra in the 500–2000  $\text{cm}^{-1}$  region of the samples with a  $\text{MX}_2/\text{N}^\circ$  mole ratio of 2.00/1 and free surfactant: a) free surfactant, b)  $[\text{Ni}(\text{H}_2\text{O})_6](\text{NO}_3)_2$ , c)  $[\text{Co}(\text{H}_2\text{O})_6](\text{NO}_3)_2$ , d)  $[\text{Zn}(\text{H}_2\text{O})_6](\text{NO}_3)_2$ , and e)  $[\text{Cd}(\text{H}_2\text{O})_4](\text{NO}_3)_2$ .

of the surfactant, show a shift to a lower energy upon the formation of hydrogen bonds between the EO units of the non-ionic surfactant and the metal aqua complexes. Another reason for the shift to lower energy is likely a result of the symmetric stretching of the  $\text{NO}_3^-$  counterion<sup>[22]</sup> which also absorbs in this region of the spectrum. The doubly degenerate  $\text{NO}_3^-$  asymmetric stretching, which splits into two peaks at around 1300  $\text{cm}^{-1}$  and 1460  $\text{cm}^{-1}$ , displays visible changes from complex to complex. These two peaks show variation in their frequencies from metal to metal and are most likely a result of the  $\text{NO}_3^-$  ion interacting with the surfactant and metal aqua complexes. Note that the FT-IR spectra of the  $[\text{M}(\text{H}_2\text{O})_n](\text{NO}_3)_2$  salts display a characteristic single peak at around 1385  $\text{cm}^{-1}$ , and the free nitrate ion displays a very broad peak at around 1400  $\text{cm}^{-1}$ . It is clear from our observations that upon introducing these salts into the surfactant both the dissociated  $\text{NO}_3^-$  (free nitrate ion) and associated  $\text{NO}_3^-$  ions (ion-pair) coexist with the metal aqua complex. The peak at around 945  $\text{cm}^{-1}$  and the broad feature

at around 930  $\text{cm}^{-1}$  are characteristic of the *gauche* and *trans* forms, respectively, of the ethylene oxide (EO) units of the surfactant.<sup>[23]</sup> [18]crown-6 is one of the molecules in which all of the EO groups are in a *gauche* form and which displays a very sharp peak<sup>[24]</sup> at 945  $\text{cm}^{-1}$ . However, disordered poly(ethylene oxide)- and oligo(ethylene oxide)-type surfactants mostly display the peak corresponding to the *trans* form.<sup>[23]</sup> The *gauche* form, we believe, is the major structural type, which organizes the surfactant molecules into the hexagonal and/or cubic LC phases. The characteristic peak at 945  $\text{cm}^{-1}$ , which is attributed to the *gauche* form of the EO units, is more intense for the Cd(II) system (Figure 4). This result is also consistent with the observed thermal properties that show the  $[\text{Cd}(\text{H}_2\text{O})_4](\text{NO}_3)_2/\text{N}^\circ$  systems to be thermally more stable than the Co, Ni, and Zn systems.

In conclusion, we have shown that oligo(ethylene oxide)-type surfactants show LC behavior in the presence of  $[\text{M}(\text{H}_2\text{O})_n](\text{NO}_3)_m$ -type transition metal aqua complexes which function as the second component of the LLC phase. Here, the coordinated water molecules of the transition metal aqua complexes induce the aggregation and self-assembly of the surfactant molecules into hexagonal and/or cubic structures and allow the transition metal ions to be distributed into these structures uniformly in the form of free ions and ion pairs with the  $\text{NO}_3^-$  counterion.

#### Experimental Section

The samples were prepared by mixing the surfactant and the salts of metal complexes in a solid phase. 10-lauryl ether (1 g, ca.  $1.6 \times 10^{-3}$  mol) was mixed with the metal salts in the  $\text{MX}_2/\text{N}^\circ$  mole ratios of 0.1/1–7.0/1. The mixtures were homogenized by heating over their IT and cooling with constant shaking. These heating and cooling cycles were repeated several times to achieve homogeneity. Finally, the samples were kept under their ITs for several to 24 h. This is a crucial step to ensure that the metal ions are homogeneously distributed; otherwise one may obtain different isotropization temperatures for different measurements on the same sample. However, over-heating, especially in the case of  $[\text{Cd}(\text{H}_2\text{O})_4](\text{NO}_3)_2$  samples, may destroy the desired LC phase. The new phases, obtained upon homogenizing, are transparent and have the color of the complex ion. They display optical-fan textures between the cross polars under POM.

The POM images were recorded in transmittance mode on a stereo microscope Stemi 2000 from Carl Zeiss Jena GmbH and on a Meije Techno ML9400 series polarizing microscope with transmitted light illumination, by using convergent white light between parallel and crossed polarizers. The thermal properties of the mixtures were studied using a Leica Microscope Heating Stage 350 attached to the above microscope. The X-ray diffraction (XRD) patterns were obtained on a Rigaku Miniflex diffractometer using a high-power  $\text{Cu}_{\text{K}\alpha}$  source operating at 30 kV/15 mA. FT-IR spectra were recorded from thin films deposited between two Si(100) wafers on a BOMEM 102 FT-IR spectrometer in transmittance mode. UV/Vis absorption spectra were recorded from film samples prepared on quartz windows by using a Varian Cary 5 double-beam spectrophotometer.

Received: May 23, 2001  
Revised: July 30, 2001 [Z17169]

- [1] C. T. Kresge, M. E. Leonawicz, W. J. Roth, J. C. Vartuli, J. S. Beck, *Nature* **1992**, 359, 710.
- [2] J. S. Beck, J. C. Vartuli, W. J. Roth, M. E. Leonawicz, C. T. Kresge, K. T. Schmitt, C. T.-W. Chu, D. H. Olson, E. W. Sheppard, S. B. McCullen, J. B. Higgins, J. L. Schlenker, *J. Am. Chem. Soc.* **1992**, 114, 10834.

- [3] I. Soten, G. A. Ozin, *Curr. Opin. Colloid Interface Sci.* **1999**, *4*, 325.
- [4] J. Y. Ying, C. P. Mehnert, M. S. Wong, *Angew. Chem.* **1999**, *111*, 58; *Angew. Chem. Int. Ed.* **1999**, *38*, 56.
- [5] H. Winkler, A. Brinkner, V. Hagen, I. Wolf, R. Schmechel, H. Seggern, R. A. Fischer, *Adv. Mater.* **1999**, *11*, 1444.
- [6] H. Yang, N. Coombs, I. Sokolov, G. A. Ozin, *Nature* **1996**, *381*, 589.
- [7] P. Yang, D. Zhao, B. F. Chmelka, G. D. Stucky, *Chem. Mater.* **1998**, *10*, 2033.
- [8] B. T. Holland, C. F. Blanford, A. Stein, *Science* **1998**, *281*, 538; G. A. Ozin, S. M. Yang, *Adv. Funct. Mater.* **2001**, *11*, 95.
- [9] G. S. Attard, J. C. Glyde, C. G. Göltner, *Nature* **1995**, *378*, 366.
- [10] P. V. Braun, P. Osenar, S. I. Stupp, *Nature* **1996**, *380*, 325; P. Osenar, P. V. Braun, S. I. Stupp, *Adv. Mater.* **1996**, *8*, 1022; P. V. Braun, P. Osenar, V. Tohver, S. B. Kennedy, S. I. Stupp, *J. Am. Chem. Soc.* **1999**, *121*, 7302.
- [11] X. Jiang, Y. Xie, J. Lu, L. Zhu, W. He, Y. Qian, *Chem. Mater.* **2001**, *13*, 1213.
- [12] G. S. Attard, C. G. Göltner, J. M. Corker, S. Henke, R. H. Templer, *Angew. Chem.* **1997**, *109*, 1372; *Angew. Chem. Intl. Ed. Engl.* **1997**, *36*, 1315; G. S. Attard, P. N. Bartlett, N. R. B. Coleman, J. M. Elliott, J. R. Owen, J. H. Wang, *Science* **1997**, *278*, 838; A. H. Whitehead, J. M. Elliott, J. R. Owen, G. S. Attard, *Chem. Commun.* **1999**, 331; G. S. Attard, S. A. A. Leclerc, S. Maniguet, A. E. Russell, I. Nandhakumar, P. N. Bartlett, *Chem. Mater.* **2001**, *13*, 1444.
- [13] S. Eftekhazadeh, S. I. Stupp, *Chem. Mater.* **1997**, *9*, 2059.
- [14] Ö. Dag, A. Verma, G. A. Ozin, C. T. Kresge, *J. Mater. Chem.* **1999**, *9*, 1475.
- [15] O. Samarskaya, Ö. Dag, *J. Colloid Interface Sci.* **2001**, *238*, 203.
- [16] G. S. Attard, P. N. Bartlett, N. R. B. Coleman, J. M. Elliott, J. R. Owen, *Langmuir* **1998**, *14*, 7340.
- [17] D. J. Mitchell, G. J. T. Tiddy, L. Waring, T. Bostock, M. P. McDonald, *J. Chem. Soc. Faraday Trans.* **1983**, *79*, 975; P. Sakya, J. M. Seddon, R. H. Templer, R. J. Mirkin, G. J. T. Tiddy, *Langmuir* **1997**, *13*, 3706.
- [18] V. Percec, D. Tomazos, J. Heck, H. Blackwell, G. Ungar, *J. Chem. Soc. Perkin Trans.* **1994**, *2*, 31; M. Lee, B.-K. Cho, *Chem. Mater.* **1998**, *10*, 1894; T. Ohtake, M. Ogasawara, K. Ito-Akita, N. Nishina, S. Ujiie, H. Ohno, T. Kato, *Chem. Mater.* **2000**, *12*, 782.
- [19] F. A. Cotton, G. Wilkinson, *Advanced Inorganic Chemistry*, 5th ed., Wiley, New York, **1988**, p. 727; J. E. Huheey, E. A. Keiter, R. L. Keiter, *Inorganic Chemistry: Principles of Structure and Reactivity*, 4th ed., Harper Collins, New York, **1993**, p. 433.
- [20] R. G. Laughlin, *The Aqueous Phase Behaviour of Surfactants*, Academic Press, San Diego, **1987**.
- [21] H. Yang, A. Kuperman, N. Coombs, S. Mamiche-Afara, G. A. Ozin, *Nature* **1996**, *379*, 703; H. Yang, N. Coombs, I. Sokolov, G. A. Ozin, *J. Mater. Chem.* **1997**, *7*, 1285; H. Miyata, K. Kuroda, *Chem. Mater.* **1999**, *11*, 1609; H. Miyata, K. Kuroda, *Chem. Mater.* **2000**, *12*, 49.
- [22] J. Laane, J. R. Ohlsen, *Prog. Inorg. Chem.* **1986**, *28*, 465.
- [23] N. Kimura, J. Umemura, S. Hayashi, *J. Colloid Interface Sci.* **1996**, *182*, 356.
- [24] B. Schrader, *Raman/Infrared Atlas of Organic Compounds*, 2nd ed., VCH, Weinheim, **1984**, p. J7.

## Photoluminescent Silicate Microsticks Containing Aligned Nanodomains of Conjugated Polymers by Sol–Gel-Based In Situ Polymerization\*

Takuzo Aida\* and Keisuke Tajima


Polymeric materials with unidirectionally aligned nanodomains of conjugated polymers are expected to have potential for novel electroconductive and optoelectronic devices.<sup>[1]</sup> In this respect, template-assisted polymerizations in organized media have attracted much attention.<sup>[2, 3]</sup> An attractive approach is to utilize mesoporous inorganic materials with ordered hexagonal arrays of uniformly sized nanoscale channels.<sup>[4]</sup> Bein et al. reported the synthesis of a graphite-type conducting carbon nanowire by free-radical polymerization of acrylonitrile within the silicate channels of MCM-41, followed by pyrolysis of the resulting polymer.<sup>[5]</sup> More recently, Cardin et al. reported Ni<sup>II</sup>-catalyzed polymerization of alkynes inside the silicate channels of MCM-41 to give polyynes/silica hybrid composites.<sup>[6]</sup> On the other hand, Tolbert et al. reported the synthesis of photoluminescent polymer/silica hybrids by loading poly(phenylene vinylene) derivatives into pre-formed mesoporous silicate channels.<sup>[7]</sup> However, because of adsorption, such post-loading approaches may not always guarantee complete filling of the nanoscopic channels with functional guests. Hence, new strategies are required for the synthesis of well-defined composite materials from conjugated polymers and nanostructured silicates.

We have reported some unique approaches toward controlled macromolecular synthesis using mesoporous silicate materials.<sup>[8–10]</sup> Here we report on the fabrication of novel micrometer-scale photoluminescent silicate sticks with segregated nanodomains of conjugated polymers by sol–gel-based in situ polymerization of diacetylenic surfactant monomers **1**, which were then used as templates for the formation of mesostructured silicates (Scheme 1). This method is expected to allow complete filling of the silicate channels with ordered diacetylenic monomers **2**. Such a dense packing of the monomer is essential for the polymerization of **1** within the silicate channel, since diacetylene derivatives can only be polymerized topochemically in condensed crystalline and semi-crystalline phases.<sup>[11]</sup>

The template surfactant monomers 2,4-, 5,7-, and 9,11-hexadecadiynyltrimethylammonium bromides **1a–1c** were synthesized by a Cadiot–Chodkiewicz coupling reaction of

[\*] Prof. Dr. T. Aida, K. Tajima  
Department of Chemistry and Biotechnology  
Graduate School of Engineering  
The University of Tokyo  
7-3-1 Hongo, Bunkyo-ku, Tokyo 113-8656 (Japan)  
Fax: (+81)3-5841-7310  
E-mail: aida@macro.t.u-tokyo.ac.jp

[\*\*] K.T. thanks the Japan Society for the Promotion of Science (JSPS) for a Young Scientist Fellowship.

 Supporting information for this article is available on the WWW under <http://www.angewandte.com> or from the author.